Machinablity analysis and optimisation of process paramater in the turining of Inconel 718 alloy using multi criteria decision making method: A comparative study

Qian Zhou
Vinothkumar Sivalingam (svkceg@gmail.com)
Shandong University https://orcid.org/0000-0002-6705-5933
Karthik Pandiyan
Ganesh Kumar
Jie Sun

Research Article

Keywords: Inconel 718 alloy, Turning, Multi-criteria decision making (MCDM), surface roughness, tool life, Vibration acceleration, TOPSIS method, CODAS method, EDAS method

Posted Date: April 21st, 2022

DOI: https://doi.org/10.21203/rs.3.rs-1542507/v1

Abstract

Manufacturing sectors strive towards low-toxic, environmentally friendly machining to combat climate change. Due to its low heat conductivity, machining Inconel 718 alloy is a difficult process nowadays. The purpose of this research is to investigate the turning of Inconel 718 alloy under PVD TiAlN inserts in two distinct environments: dry and atomized spray cutting fluid (ASCF). The effect of various machining performance such as surface roughness(R_a), vibration acceleration (VA), and tool life (TL) analysis of Inconel 718 alloy in ecologically friendly machining were investigated in this study. Further, Multicriteria decision-making (MCDM) was used to find best optimal process settings: TOPAIS (Technique for Ordering Performance by Similarity to Ideal Solution), CODAS (Combinative Distance-Based Assessment Technique), and EDAS (Evaluation Based on Distance from Average Solution) are three techniques for evaluating performance by similarity to ideal solution. In an ASCF setting, the MCDM approach yields comparable results with an ideal cutting speed (v_c) of 50 m/min, feed rate (f) of 0.15 mm/rev, and depth of cut (a_p) of 0.4mm. In contrast to dry machining, ASCF machining yielded a 17–34% improvement in surface quality. In dry circumstances, the crater and chipping processes were obvious in the rake face, although less wear was noticed in ASCF machining. Because the thermal conductivity of cutting fluids is improved by microscopic droplets of ASCF, rapid heat dissipated from the machining zone.

1. Introduction

Due to excellent heat resistance, about 50% of Inconel 718 alloy is consumed in jet engine components and gas turbine blades. [1]. The lack of heat conductivity and strong mechanical characteristics of Inconel 718 alloy have a considerable impact on machinability throughout the manufacturing process [2]. When turning or milling Inconel 718 alloys, high cutting temperatures created at the workpiece – tool interface (turning or milling) cause chemical reactions with the cutting inserts. These are the primary concerns when turning or milling Inconel 718 alloys. [3]. Once the cutting speed (v_c) exceeds about 100 m/min, the cutting pressures and temperatures at the machined region grow rapidly, resulting in thermal softening or thermal cracking [4, 5]. These characteristics result in increased v_c and energy consumption, which can decrease tool life and cause major surface and subsurface flaws in machine-induced surfaces [6]. Novel cooling techniques such as MQL (minimum quantity lubrication), ASCF (Atomised spray cutting fluid), ASFC with nanofluids (Solid lubricants), cryogenic cooling, and others have been proposed as a viable alternatives to enhance the machinability and tribological properties of Inconel 718 alloy [7]. They're called "Green machining" because of the beneficial results. Because the cutting fluid consumption in these cooling systems is rather modest, the environmental impacts are negligible in this case [8]. The ASCF technique is utilised in virtually all conventional machining operations, to control tool failure and optimise the machining performance surface. The ASCF concept arose from a desire to significantly enhance the surface integrity and extend tool life with minimal coolant usage in turning applications [9]. Elsheikh et al. [10] investigated the effects of the MQL method on AISI 4340 steel turning with cermet inserts utilising nanoparticles (Al_2O_3 and CuO). CuO added nano-fluids outperform Al_2O_3 added nano-fluids enhances the surface integrity and extend tool wear, according to the researchers, due to CuO's stronger thermal properties. During the machining of pure titanium, Singh et al.[11] examined the v_c, surface roughness (R_a), and tool wear parameters of a chilled air

assisted with MQL. The usage of chilled air aided MQL enhanced the surface quality of several hard-to-cut materials and lowered the risk of occupational health hazards, according to the authors. Chetan et al. [12] machined Nimonic 90 superalloy with carbide inserts and in comparison with cryogenic cooling and nano-MQL techniques. This approach for minimising tool wear was found to be cryogenic cooling. Furthermore, in connection with tool wear and surface quality, the nano-MQL technique surpasses cryogenic treatment. Sivalingam et al. [13] use the ASCF technique applied in machining of Inconel 718 alloy in turning application by using vegetable oil mixed with graphite and molybdenum disulphide. The purpose of this strategy is to lessen pollution's detrimental effects on the environment. Fine atomised spray fluids are distributed throughout the tool-chip contact area, subsequently decreased friction, and effective heat transport away from the cutting zone. The machine tool industry strives for increased productivity and efficiency, which are closely tied to optimal cutting settings. However, during machining of Inconel 718 alloy challenging task is to predict the optimal process parameters combination might be difficult. This can aid with tool wear, surface quality, and overall productivity [14, 15]. The multicriteria decision-making (MCDM) approach has been used by a number of researchers in a variety of fields, including supply chain management, finance, renewable energy, manufacturing, and waste water treatment [16]. Gok [17] used fuzzy TOPSIS, grey relational analysis, and Response surface analysis (RSA) to investigate the R_a and v_c throughout the turning process, and found the ideal cutting parameters to minimise v_c and enhance R_a. Analysis of variance (ANOVA) provides a way for generating a prediction model of R_a and v_c based on cutting parameters. The results demonstrate that R_a and v_c are mostly influenced by the depth of cut (a_p). Shukla et al. [18] discussed how the TOPSIS approach might be used to optimise a variety of metal cutting process, such as milling, drilling, turning, EDM, abrasive jet machining, micromachining, and other machining processes. Furthermore, the superiority of the TOPSIS algorithm was highlighted, as well as the clear improved effect on real processing. To investigate the multi-response optimization of process parameters of titanium alloy (grade 2) in the (Nano fluid) NFMQL-assisted turning process, Gupta et al. [19] integrated the TOPSIS approach with the particle swarm optimization algorithm (PSO). According to the findings, graphite based nanofluids with a v_c of 204 m/min, f of 0.11 mm/rev, nozzle angle of 75º is the best process parameters. Rao et al. [20] employed TOPSIS technology to optimise the parameters of v_c, f, and a_p, determining the optimal combination of v_c, f, and a_p. Thirumalai et al.[21] investigated multi-response optimization of Inconel 718 turning process parameters, using the NSGA-II approach to produce a set of objective functions that optimise tool life and MRR while minimising cutting force, and then ranking the solutions using the TOPSIS method. Simic et al. [22] studied the location of vehicle crusher facilities using Image Fuzzy Sets (PFSs) and suggested a multi-criteria vehicle crushing facility selection assessment combinative distance-based assessment (CODAS) technique using image fuzzy combined distance. The strategy is put to the test in real-world scenarios and compared to other MCDM approaches. The findings reveal that the strategy is quite consistent with previous approaches. Kumar et al.[23] used the intuitionistic Fuzzy Combination Distance-Based Assessment (IFCODAS) approach to apply distinct nanoparticle-based quantifications to heat exchangers, which merged the intuitionistic Fuzzy Set (IFS) theory with the (CODAS) method. Continued testing has revealed that carbon-based nanoparticles offer significant benefits in terms of delivering stable and dependable thermal systems. Badi et al.[24] applied the CODAS approach to a real-world situation and chose the finest LISCO supplier in Libya. The CODAS

technique improves the efficacy of quality decision-making and makes the quality decision-making process more logical, clear, and efficient, according to the findings. Chairman et al. [25] utilised evaluation based on distance from average solution (EDAS) is MCDM technique paired with Taguchi method, to conduct a double-body abrasive wear test on glass fibre reinforced epoxy resin (GC)/titanium dioxide (TiO2) composites. According to the EDAS technique, the 2 wt% TiO_2 filled epoxy composite had the best filler content of the three weight percentages under all mechanical testing conditions. Asante et al.[26] merged the old MULTIMOORA approach with EDAS to establish a MULTIMOORA-EDAS method for evaluating renewable energy (RE) obstacles, which he then used to evaluate the hurdles to RE development.

This study presents a combined MCDM approach for selecting the best process parameter for turning Inconel 718 alloy. The following are the study's main contributions. To our knowledge, this is the first attempt to use integrated shannon entropy for determining individual weightage values, further three MCDM method namely TOPSIS, EDAS, and CODAS is used to evaluate turning paparmeters. v_c, f, and a_p are all improved when the process parameters are optimised. However, no study has been done to find the optimal process parameter by taking into account all elements in decision-making processes, such as minimising vibration, minimising surface roughness, and maximising tool life.

Using an MCDM TOPSIS, CODAS, and EDAS approach, this study seeks to identify, analyse, and optimise Inconel 718 alloy turning process parameters. The purpose of the Taguchi L18 experiment was to find the best setting for R_a, vibration acceleration (VA), and tool life (TL). These studies suggest an integrated MCDM approach for determining optimal process parameters.

2. Materials And Methods

All of the turning experiments were carried out on DAEWOO PUMA-2000 CNC turning machining. The workpiece was machined using a PVD (TiAlN + $AlCr_2O_3$) coated carbide insert with ISO number SNMG 120408 – Sandvik. Table 1 shows all of the experimental work in detail. In this study, vegetable oil mixed with solid lubricant (graphite and molybdenum disulphide) additives is utilised the ASCF machining to explore the effect of solid lubricating cooling in the turning application. To illustrate the advantages of the ASCF technique, dry machining is also used. Producer for preparation of solid lubricant first take 20ml of acetone and added 0.2 wt. % of each solid additives (graphite and molybdenum disulphide) is blended to ensure homogenous particle dispersion. After that, a 90:10 mixture of cutting fluid and solid lubricant is applied. The atomised nozzle consists of two input one is used to supply air pressure of 7 bar and other side solid lubricating flow of 30 mL/h is maintained by adjustable screw. The distance between the atomised nozzle and the cutting insert is regulated at 50 mm during machining. For each trial, a fresh cutting edge was employed to accurately analyse machining performance. A magnetic holder holds the vibration sensor to the tool holder. Veeco NT 9300 white light interferometer non-contact type 2D surface roughness measurement was used. For each cutting condition, a TR200 portable surface roughness profilometer was employed for average surface roughness (R_a). The dry and ASCF processes are depicted schematically in Fig. 1. The experimental value is shown in Table 2.

Table 1
Experimental Conditions

Instruments	Details
Workpiece	Inconel 718 alloy (Ø80 X 400 mm) Chemical Composition (% weight) – Ni (53), Cr (18), C (0.04), Mn (0.08), Si (0.08), Co (0.23), Mo (3.04) Nb (5.3), Ti (0.98), Al (0.50), Fe (17.80) Mechanical Properties – Tensile strength (1170 MPa), Yield strength (1375 MPa), Elongation (23.3%), Hardness (40 HRC).
Cutting speed (v_c)	50, 75 and 100 m/min
Feed rate (f)	0.1, 0.15 and 0. 2 mm/rev
Depth of cut (a_p)	0.4, 0.8 and 1.2mm
Length of cut (Loc)	40 mm
Optical Light Microscope	Keyence VH- Z500R magnification (500 – x 5000)
Vibration sensor	PCB 356A15 acceleration sensor

Table 2
Experimental data

Exp.No	Environment	Cutting Speed	Feed rate	Depth of cut	SR	VB	Tool life (TL)
		m/min	mm/rev	mm	mm	m/s^2	min
1	1	50	0.1	0.4	0.685	0.119	17
2	1	50	0.15	0.8	0.87	0.196	15
3	1	50	0.2	1.2	1.291	0.358	12
4	1	75	0.1	0.4	0.722	0.143	12
5	1	75	0.15	0.8	0.919	0.235	14
6	1	75	0.2	1.2	1.291	0.378	12
7	1	100	0.1	0.8	0.898	0.218	12
8	1	100	0.15	1.2	1.012	0.332	12
9	1	100	0.2	0.4	1.11	0.248	11
10	2	50	0.1	1.2	0.867	0.21	26
11	2	50	0.15	0.4	0.623	0.095	25
12	2	50	0.2	0.8	0.853	0.162	21
13	2	75	0.1	0.8	0.698	0.123	20
14	2	75	0.15	1.2	0.978	0.275	23
15	2	75	0.2	0.4	0.745	0.128	21
16	2	100	0.1	1.2	0.937	0.265	22
17	2	100	0.15	0.4	0.713	0.122	20
18	2	100	0.2	0.8	0.913	0.216	18
* Environment, 1 = Dry machining ; 2 = ASCF machining							

3. Multicriteria Decision-making Methodologies

3.1 Shannon Entropy Method

The Shannon entropy technique is a weighted model that uses the project outcome to determine the weights of particular criterion [27–29]. The entropy weight approach is explained as follows:

(i) To get a project outcome r_{ij},

$$r_{ij} = \frac{x_{ij}}{\sum_{i=1}^{m} x_{ij}}$$

1

(ii) Compute entropy value.

$$E_j = -k\sum_{i=1}^{m} r_{ij} \times \ln r_{ij}$$

$$k = \frac{1}{\ln(m)}$$

2

(iii) Using the entropy notion to define the objective weight

$$W_j = \frac{1 - E_j}{\sum_{j=1}^{n} (1 - E_j)}$$

3

3.2 Technique for Order Preference by Similarity to Ideal Solution (TOPSIS) method

The optimal choice is the one that is closest to the best answer and farthest away from the non-ideal alternative, according to the TOPSIS concept. [19]. The TOPSIS approach is based on an impulsive and straightforward premise. It entails selecting a good choice that is superior to the worst and obtaining a greater advantage.[30, 31] The best outcome will be given a rank, while the lowest will receive a zero. This strategy is both time-saving and cost-effective.

(1) Calculation of normalise matrix $\left(x_{ij}\right)_{m\times n}$

$$R_{ij} = \frac{x_{ij}}{\sqrt{\sum_{i=1}^{m} x_{ij}^2}}$$

4

R_{ij} - normalised performance matrix; x_{ij} - normalised value of i^{th} experimental order related to the j^{th} output variables (R_a, *VA, TL*)

(2) weighted normalized matrix

$$V_{ij} = W_j \times R_{ij}$$

5

V_{ij} - weighted normalized matrix; W_j - weighted values

(3) Positive and negative ideal solutions

$$P^{+}or\left(P^{-}\right)=\left\{\left[\max\left(P_{ij}\right)\middle|j\in J\right]or\left[\min\left(P_{ij}\right)\middle|j\in J^{'}\right],\right\} \quad (6)$$

P^+ – good performance in a different situation; P^- stands for the worst alternative performance.

(4) Best and worst alternative distance

$$D_i^+ = \sqrt{\sum_{j=1}^{m}\left(V_{ij}-P_j^+\right)^2}; D_i^- = \sqrt{\sum_{j=1}^{m}\left(V_{ij}-P_j^-\right)^2}, \forall i \quad (7)$$

D_{ij}^+ - The most suitable alternative distance; D_{ij}^- - Alternative distance with the worse results. *J*- represents the criteria that have a favourable effect; J′- identifies the characteristics that have a detrimental influence;

(5) Closeness Coefficient

$$C_i = \frac{D_i^-}{D_i^- + D_i^+}, 0 \leqslant$$

8

C_i - closeness coefficient.

3.3 Combinative Distance-based Assessment Method (CODAS)

CODAS is an innovative decision-making technique for multicriteria situations. The approach relies on the Euclidean distance in between positive and negative alternatives.[32–35]

(1) Creating a decision matrix for the first time {\left({{x_{ij}}} \right)_{m \times n}}

X={\left[{{x_{ij}}} \right]_{_{{n\,x\,m}}}}=\left[{\begin{array}{*{20}{c}} {{x_{11}}}&{{x_{12}}}&{.....}&{{x_{1m}}} \\ {{x_{21}}}&{{x_{22}}}&{.....}&{{x_{2m}}} \\ \begin{gathered} . \hfill \\ . \hfill \\ \end{gathered} &\begin{gathered} . \hfill \\ . \hfill \\ \end{gathered} &\begin{gathered} . \hfill \\ . \hfill \\ \end{gathered} &\begin{gathered} . \hfill \\ . \hfill \\ \end{gathered} \\ {{x_{n1}}}&{{x_{n2}}}&{.....}&{{x_{nm}}} \end{array}} \right] {\left({{x_{ij}}} \right)_{m \times n}} matrix (9)

R_{ij} - normalized performance matrix

(2) Normalised decision matrix.

{N_{ij}}=\left({\begin{array}{*{20}{c}} {\frac{{{x_{ij}}}}{{\mathop {\hbox{max} }\,{x_{ij}}}\limits_{i} }}&{if\,j \in Higer\,the\,better} \\ {\frac{{\mathop {\hbox{min} }\,{x_{ij}}}\limits_{i} }}{{{x_{ij}}}}&{if\,j \in Lower\,the\,better} \end{array}} \right)
10

(3) Calculation of Weighted normalize matrix

{R_{ij}}={W_j}\,{N_{ij}}
11

(4) Determine the points of the negative-ideal solution.

NS={\left[{N{S_j}} \right]_{1x\,m}},\,\,\,\,\,\,\,\,(N{S_{^{j}}}=\mathop {\hbox{min} }\limits_{i} \,\,{R_{ij}})
12

NS = negative-ideal solution.

(5) Calculation of the Euclidean and taxicab distances from ns.

{e_i}=\sqrt {\sum\limits_{{j=1}}^{m} {{{\left({{R_{ij}} - N{S_j}} \right)}^2}} } ,\,\,\,\,\,\,\,\,\,
{t_i}=\sum\limits_{{j=1}}^{m} {\left| {{R_{ij}} - N{S_j}} \right|}
13

e_i-Euclidean distances; t_i - taxicab distances

(6) Create a matrix of relative assessments.

\begin{gathered} Ra=\left[{{D_{ik}}} \right]{\,_{m\,x\,n}},\,\,\,{D_{ik}}=\left({{e_i} - {e_k}} \right)+\left({\psi \left({{e_i} - {e_k}} \right)\,X\left({{t_i} - {t_k}} \right)} \right) \hfill \\ \left({Assume,\,\psi =0.02\,} \right) \hfill \\ \end{gathered}
14

(7) Calculation of relative assessment score.

{H_i}=\sum\limits_{{k=1}}^{n} {{D_{ik}}}
15

3.4 Evaluation based on Distance from average solution (EDAS)

The difference between distinct process parameters in this model may be evaluated using the appraisal score (AS), which is based on a positive distance from average (PDA) and a negative distance from average (NDA) (NDA). The best parameters have the highest PDA values and the lowest NDA values. [27, 36–38]

(1) Calculation of the initial decision matrix {\left({{x_{ij}}} \right)_{m \times n}}

X={\left[{{x_{ij}}} \right]_{_{{n\,x\,m}}}}=\left[{\begin{array}{*{20}{c}} {{x_{11}}}&{{x_{12}}}&{.....}&{{x_{1m}}} \\ {{x_{21}}}&{{x_{22}}}&{.....}&{{x_{2m}}} \\ \begin{gathered} . \hfill \\ . \hfill \\ \end{gathered} &\begin{gathered} . \hfill \\ . \hfill \\ \end{gathered} &\begin{gathered} . \hfill \\ . \hfill \\ \end{gathered} &\begin{gathered} . \hfill \\ . \hfill \\ \end{gathered} \\ {{x_{n1}}}&{{x_{n2}}}&{.....}&{{x_{nm}}} \end{array}} \right]
16

(2) Average solution

A{S_j}=\frac{{\sum\limits_{{i=1}}^{n} {{x_{ij}}} }}{n}
17

AS $_j$ – Average solution;

(3) Distance from the average PDA is positive.

PD{A_{ij}}=\left({\begin{array}{*{20}{c}} {\frac{{\hbox{max} (0,({x_{ij}} - A{S_j}))}}{{\mathop {A{S_j}}\limits_{{}} }}}&{if\,j \in Higher\,the\,better} \\ {\frac{{\hbox{max} (0,(A{S_j} - {x_{ij}}))}}{{A{S_j}}}}&{if\,j \in Lower\,the\,better} \end{array}} \right)
18

(4) Distance from the average NDA that is negative.

ND{A_{ij}}=\left({\begin{array}{*{20}{c}} {\frac{{\hbox{max} (0,(A{S_j} - {x_{ij}}))}}{{\mathop {A{S_j}}\limits_{{}} }}}&{if\,j \in Higher\,the\,betterl} \\ {\frac{{\hbox{max} (0,({x_{ij}} - A{S_j}))}}{{A{S_j}}}}&{if\,j \in Lower\,the\,better} \end{array}} \right)
19

(5) SP and SN normalised values

\begin{gathered} NS{P_i}=\frac{{S{P_i}}}{{{{\hbox{max} }_i}(S{P_i})}}\sum\limits_{{j=1}}^{m} {{w_j}*PD{A_{ij}}} \hfill \\ NS{N_i}=1 - \frac{{S{N_i}}}{{{{\hbox{max} }_i}(S{N_i})}}\sum\limits_{{j=1}}^{m} {{w_j}*PD{A_{ij}}} \hfill \\ \end{gathered}
20

(6) Appraisal Score

A{S_i}=\left[{\frac{{NS{P_i}+NS{N_i}}}{2}} \right]
21

4. Result And Discussion

In this study, we conducted a turning experiment and defined the input machine variables such as v_c, f, and a_p, as well as output criteria such as surface roughness (SR), vibration acceleration (VA), and tool life (TL), in order to optimise the process parameter. We employed three MCDM models, TOPSIS, CODAS, and EDAS, to rank the options with regard to the given criteria in this study in order to find the best process parameter. As previously stated, the weights of the criterion are determined using the Entropy technique. We utilise the decision matrix described in the Entropy technique and then normalise decision matrix (r_{ij}) it is using Eq. (1). We next use Eq. (2) to determine the entropy of each criterion, which is represented by E_j. Using Eq. (3), we derive the weights of each criterion, indicated by W_j. The weightage of each criterion W_j for SR, VA and TL is 0.154, 0.557 and 0.289 respectively.

The normalised matrix values for different TOPSIS process parameters were determined using Eq. (9), and the normalised values are shown in Table 3. By considering performance aspects: Lower the better (LB) is preferable for SR and VA, higher is better for TL. We may generate a weighted normalised matrix by multiplying the entropy weighting value with Eq. 9. We get weighted normalised matrix ({V_{ij}}).

Table 3
Closeness coefficient values of TOPSIS analysis

Exp.No	Normalized Decision Matrix			Weighted Normalized Decision Matrix			D_i^+	D_i^-	C_i	Rank
	SR	VA	TL	SR	VA	TL				
	mm	m/s^2	min	mm	m/s^2	min				
1	0.176	0.123	0.222	0.027	0.068	0.064	0.037	0.153	0.807	5
2	0.224	0.202	0.196	0.035	0.113	0.057	0.072	0.108	0.599	9
3	0.333	0.370	0.157	0.051	0.206	0.045	0.162	0.013	0.072	17
4	0.186	0.148	0.157	0.029	0.082	0.045	0.060	0.138	0.698	7
5	0.237	0.243	0.183	0.037	0.135	0.053	0.093	0.085	0.477	12
6	0.333	0.391	0.157	0.051	0.218	0.045	0.174	0.004	0.021	18
7	0.231	0.225	0.157	0.036	0.125	0.045	0.089	0.094	0.514	11
8	0.261	0.343	0.157	0.040	0.191	0.045	0.147	0.029	0.167	16
9	0.286	0.256	0.144	0.044	0.143	0.041	0.106	0.076	0.416	15
10	0.223	0.217	0.339	0.034	0.121	0.098	0.067	0.114	0.630	8
11	0.160	0.098	0.326	0.025	0.055	0.094	0.004	0.174	0.979	1
12	0.220	0.167	0.274	0.034	0.093	0.079	0.044	0.131	0.750	6
13	0.180	0.127	0.261	0.028	0.071	0.075	0.028	0.153	0.845	4
14	0.252	0.284	0.300	0.039	0.158	0.087	0.105	0.076	0.419	14
15	0.192	0.132	0.274	0.030	0.074	0.079	0.027	0.151	0.847	2
16	0.241	0.274	0.287	0.037	0.153	0.083	0.100	0.079	0.440	13
17	0.184	0.126	0.261	0.028	0.070	0.075	0.028	0.153	0.847	3
18	0.235	0.223	0.235	0.036	0.124	0.068	0.077	0.098	0.562	10

Each alternative experiment's the positive and negative ideal distance solution values were computed using Eq. (7). Using the D_{{ij}}^{+}, D_{{ij}}^{ - } values, the closeness coefficient index (C_i) was determined for each alternative using Eq. (8). The values of the proximity coefficients for each experimental run utilising the L18 orthogonal array are shown in Table 3. Because it indicates the highest proximity coefficient; the values recorded in each trial, from the 18 closeness coefficients showed that experiment 11 had the best multi-response characteristics. Experiment no. 11 yielded optimal process settings in the MCDM methods for the output responses this will conformed with higher C_i values indicates the best setting for the Inconel 718 alloy machining.

The CODAS technique uses a two-step rating procedure to assess the attractiveness of particular traits. Calculate e_i and t_i distances using the *NS* [32–34, 39]. The normalised and weightage normalised performance values for each criterion are calculated using Eqs. 9–11. Eq. 12 is then used to determine the *NS*. Based on the *NS*, Eq. 13 offers two options: e_i and t_i distances. As indicated in Table 4, Eqs. 14–15 were used to generate the relative assessment matrix (Hi) and ranking scores. Because it represents the highest relative assessment core; the values recorded in each trial, highest relative assessment score value of (7.166) is consider as the best parameter settings and corresponding experiment no. 11.

Table 4
Relative assessment matrix of CODAS method

Exp.No	Normalized Decision Matrix			Weighted Normalized Decision Matrix			Negative- ideal solution		Relative Assessment matrix (H_i)	Rank
							Ei	Ti		
	SR	VB	TL	SR	VA	TL				
	mm	m/s^2	min	mm	m/s^2	min				
1	0.909	0.798	0.654	0.140	0.445	0.189	0.319	0.437	3.291	2
2	0.716	0.485	0.577	0.110	0.270	0.167	0.142	0.211	-0.295	10
3	0.483	0.265	0.462	0.074	0.148	0.133	0.014	0.019	-1.916	17
4	0.863	0.664	0.462	0.133	0.370	0.133	0.238	0.300	1.433	6
5	0.678	0.404	0.538	0.105	0.225	0.155	0.097	0.149	-0.982	14
6	0.483	0.251	0.462	0.074	0.140	0.133	0.011	0.011	-1.927	18
7	0.694	0.436	0.462	0.107	0.243	0.133	0.109	0.147	-0.786	13
8	0.616	0.286	0.462	0.095	0.159	0.133	0.031	0.051	-1.774	16
9	0.561	0.383	0.423	0.087	0.213	0.122	0.075	0.086	-1.211	15
10	0.719	0.452	1.000	0.111	0.252	0.289	0.204	0.315	0.806	8
11	1.000	1.000	0.962	0.154	0.557	0.278	0.452	0.653	7.166	1
12	0.730	0.586	0.808	0.113	0.327	0.233	0.221	0.336	1.137	7
13	0.893	0.770	0.769	0.138	0.429	0.222	0.312	0.452	3.185	4
14	0.637	0.345	0.885	0.098	0.192	0.255	0.145	0.210	-0.244	9
15	0.836	0.742	0.808	0.129	0.413	0.233	0.300	0.439	2.899	5
16	0.665	0.358	0.846	0.103	0.199	0.244	0.139	0.210	-0.353	11
17	0.874	0.779	0.769	0.135	0.434	0.222	0.316	0.454	3.275	3
18	0.682	0.440	0.692	0.105	0.245	0.200	0.134	0.214	-0.431	12

A novel and efficient MCDM technique is (EDAS). In this strategy, the attractiveness of alternatives is measured by their distance from an average answer [27, 36, 40]. The EDAS approach may be efficient for solving the turning of Inconel 718 alloy using graphite mixed lubricating oil and process parameters were adjusted since the average solution is determined by an arithmetic mean.

Eqs. 1 and 2 are used to obtain the starting matrix and average solution (16–17). Based on the criteria type, Eqs. (18) and (19) were utilised to determine positive and negative distances (PDA, NDA). The second step was to calculate the weighted total of the positive and negative distances from the average response (SPi, SNi). These figures were calculated using Eq. (20). Eq. 21 utilises the final evaluation score (AS_i) to rank the optimal process parameter based on the values of SPi and SNi, as shown in Table 5. Because it represents the highest relative assessment core; the values recorded in each trial, experiment no. 11 demonstrated the best multi-response characteristics among the values of the L18 the appraisal score (AS_i). surprise, Experiment no. 11 shows the best parameter settings, with a larger Appraisal score value indicating that the related experiment is closer to the normalized values of SP and SN value. In all three MCDM method, It has been discovered that maintaining the best parameter configuration of environment (2 i.e. ASCF), at V_c, f *and* a_p were 50 m/min, 0.15 mm, and 0.4 mm respectively results in greater values of proximity coefficient, decreasing the SR, VA, and maximizing the TL.

Table 5
Evaluation based on Distance from average solution EDAS

Exp.No	Positive distance from average PDA			Negative distance from average NDA			NSP	NSN	Appraisal Score	Rank
	SR	VA	TL	SR	VA	TL				
	mm	m/s^2	min	mm	m/s^2	min				
1	0.235	0.440	0.000	0.000	0.000	0.022	0.521	0.985	0.753	5
2	0.029	0.078	0.000	0.000	0.000	0.137	0.082	0.910	0.496	12
3	0.000	0.000	0.000	0.441	0.685	0.310	0.000	0.064	0.032	17
4	0.194	0.327	0.000	0.000	0.000	0.310	0.402	0.798	0.600	8
5	0.000	0.000	0.000	0.026	0.106	0.195	0.000	0.787	0.394	13
6	0.000	0.000	0.000	0.441	0.783	0.310	0.000	0.000	0.000	18
7	0.000	0.000	0.000	0.002	0.026	0.310	0.000	0.780	0.390	14
8	0.000	0.000	0.000	0.130	0.562	0.310	0.000	0.347	0.173	16
9	0.000	0.000	0.000	0.239	0.167	0.367	0.000	0.496	0.248	15
10	0.032	0.012	0.495	0.000	0.000	0.000	0.416	1.000	0.708	6
11	0.305	0.553	0.438	0.000	0.000	0.000	1.000	1.000	1.000	1
12	0.048	0.238	0.208	0.000	0.000	0.000	0.381	1.000	0.690	7
13	0.221	0.419	0.150	0.000	0.000	0.000	0.610	1.000	0.805	2
14	0.000	0.000	0.323	0.092	0.295	0.000	0.249	0.748	0.499	11
15	0.168	0.398	0.208	0.000	0.000	0.000	0.597	1.000	0.799	4
16	0.000	0.000	0.265	0.046	0.249	0.000	0.205	0.808	0.506	9
17	0.204	0.426	0.150	0.000	0.000	0.000	0.602	1.000	0.801	3
18	0.000	0.000	0.035	0.019	0.016	0.000	0.027	0.977	0.502	10

4.1 Surface roughness (R_a)

Dry machining roughness ranges from 0.685 to 1.291 µm, whereas ASCF machining roughness ranges from 0.698 to 0.978 µm. Increasing the f causes the R_a value to rise throughout the machining process. At a V_c of 50 m/min, f of 0.15 mm, and a_p of 0.4 mm, ASCF machining lowers roughness by 19 to 33 percent compared to dry machining. This is due to the presence of solid lubricants in the tool tip contact, which minimises the amplitude of waviness on the machined surface while maintaining a uniform profile surface as viewed in 2D. [41] Fig. 2 shows the presence of feed marks and scratches on the surface morphology.

Figure 2 depicts an optical microscopic examination of a machined surface at the ideal conditions V_c of 50 m/min, f of 0.15 mm/min, and a_p of 0.4 mm in both dry and ASCF conditions. When compared to ASCF machining, dry machining produced more grove markings and burned marks. This is due to the presence of solid lubrication, which improves heat absorption and lowers build-up edge (BUE)development.[42]

When compared to the ASCF state, the machined surface has a non-uniform surface profile with a greater value of R_a. Surface roughness was a smooth, uniform surface profile without any appearance of waviness at the beginning stage of machining in both the dry and ASCF machining environment. During dry machining, chipping and BUE cause a greater value of surface roughness on the machined surface. Dry machining creates more feed marks on the workpiece surface than ASCF machining because of the lower V_c and f. This is due to BUE being formed as a result of the long engagement of chip with cutting inserts relatively large cutting temperature generated near the cutting edge at the higher feed rate [43, 44]. Low groove markings and improved R_a on the machined surface are achieved with constructive chip breakability and decreased BUE during ASCF machining. Figure 3 depicts a 2D surface analysis of a machined surface at the ideal conditions V_c of 50 m/min, f of 0.15 mm/min, and a_p of 0.4 mm in both dry and ASCF conditions. The figure shows that in the dry state, there were more feed marks with non-uniform surface profiles, which is attributable to vibration build-up during the machining process. Surface roughness has a direct link with vibration build-up. The presence of solid lubricants droplets on the tooltip interface reduces the amplitude of waviness on the machined surface with a uniform profile surface as seen in the 2D surface at the optimum condition V_c of 50 m/min, f of 0.15 mm/min, and a_p of 0.4 mm at both dry and ASCF condition, as seen in the images.[45].

4.2 Tool life

In dry machining, higher V_c causes greater plastic deformation at the tool-workpiece contact, resulting in shorter tool life. The presence of small spray droplets of solid lubricants during machining in ASCF minimises the coefficient of friction along the workpiece and the cutting edge, reducing cutting edge sharpness during machining at high temperatures. In contrast to dry machining conditions, ASCF machining extends tool life by up to 40%-60%. Figure 4 illustrates the SEM analysis of tool wear at the optimal conditions of 50 m/min cutting speed, 0.15 mm/min feed rate, and 0.4 mm depth of cut in both dry and ASCF conditions. Craters and chipping were evident on the tool surface due to tool wear in both dry and ASCF machining environments. In the dry condition, more craters and chipping were found on the surface due to the tool and work interface at higher speeds, whereas in the ASCF condition, fewer craters and chipping were found on the surface due to the presence of solid lubricants during the machining process, resulting in a lower tool wear rate. During the turning of the workpiece in both dry and ASCF conditions, the adhesive chipping layer was visible on the rake surface of the tool.[46, 47] When opposed to dry machining, ASCF displays less crater wear and chippings due to the presence of high thermal stress and high strain hardening rate during the machining process.[42, 45, 48, 49]. The finding is also in line with that of An et al. [50] and pal et al.[51] Solid lubricants provide a cooling effect, which lowers the cutting tool temperature at the interface zone and increases tool life. ASCF machining demonstrates less substantial fracture and

diffusion area, and the damage is significantly smaller owing to solid lubrication, which minimises the heat created during the machining process and results in longer tool life.

5. Conclusions

Utilizing TOPSIS, CODAS, and EDAS methodologies, this study analyses the usage of dry and atomized spray cutting fluid (ASCF) in turning Inconel 718 alloy using coated carbide inserts.

1. The TOPSIS, CODAS, and EDAS MCDM models indicated that experiment 11 is ranked highest, followed by experiment 6 at the bottom. Despite the fact that all MCDM approaches yield the same results, TOPSIS and EDAS need less time to calculate than CODAS due to the complexity of computing the relative assessment matrix.
2. All of the MCDM approaches to maintain the optimal parameter settings of the environment (2, i.e. ASCF), V_c of 50 m/min, f of 0.15 mm/min, and a_p of 0.4 mm, with corresponding R_a, VA, and TL of 0.623μm, 0.095m/s^2, and 25 minutes, respectively. Fine droplets of ASCF machining are more successful in lowering R_a values due to their solid lubrication cooling action.
3. In contrast to dry machining, ASCF machining improved surface roughness by 17–34%. ASCF machining provides effective lubrication between the chip-tool interfaces, as well as greatly reduces the cutting temperature in the cutting zone.
4. A higher amount of craters and chipping was observed under dry conditions, whereas a lesser amount of craters and chipping were observed during the ASCF machining conditions, and there was a significant reduction of tool wear. When opposed to dry machining, ASCF machining uses a MoS_2 and graphite mixed solid lubricant that absorbs heat quickly during the machining process and provides lubrication, which minimises friction and heat at the work piece-tool interface, lowering the cutting temperature and increasing tool life.

The impact of various machining settings on quality responses might be investigated further. i.e., the impact of varying nozzle angle, nozzle distance, flow rate, and nano lubricants mixed with vegetable oil-based coolant might be investigated.

Declarations

Acknowledgments

This work is supported by Fundamental Research Funds of Shandong University **[2019HW040]**. Future for Young Scholars of Shandong University, China **(31360082064026)**.

Availability of data and material : Not applicable

Code availability: Not applicable

Conflicts of interest: The authors declare no conflict of interest.

Ethics approval: Not applicable

Consent to participate: Not applicable

Consent for publication: Not applicable

Authors' contributions

Qian Zhou: Experimental work & Data curation Writing – review & editing **Vinothkumar Sivalingam**: Conceptualization, Experimental work & Data curation Writing – review & editing, **Karthik Pandiyan:** Writing – review & editing **Ganeshkumar Poogavanam**: Writing – review & editing & Technical Validation, **Jie Sun**: Conceptualization & Supervision.

References

1. Yin Q, Liu Z, Wang B, Song Q, Cai Y (2020) Recent progress of machinability and surface integrity for mechanical machining Inconel 718: a review. Int J Adv Manuf Technol 109(1):215–245
2. Korkmaz ME, Gupta MK, Boy M, Yaşar N, Krolczyk GM, Günay M (2021) Influence of duplex jets MQL and nano-MQL cooling system on machining performance of Nimonic 80A. J Manuf Process 69:112–124
3. Grzesik W, Niesłony P, Habrat W, Sieniawski J, Laskowski P (2018) Investigation of tool wear in the turning of Inconel 718 superalloy in terms of process performance and productivity enhancement. Tribol Int 118:337–346
4. Zhang B, Njora MJ, Sato Y (2018) High-speed turning of Inconel 718 by using TiAlN-and (Al, Ti) N-coated carbide tools. Int J Adv Manuf Technol 96(5):2141–2147
5. Ezugwu E, Wang Z, Machado A (1999) The machinability of nickel-based alloys: a review. J Mater Process Technol 86(1–3):1–16
6. Erden MA, Yaşar N, Korkmaz ME, Ayvacı B, Nimel Sworna Ross K, Mia M (2021) Investigation of microstructure, mechanical and machinability properties of Mo-added steel produced by powder metallurgy method. Int J Adv Manuf Technol 114(9):2811–2827
7. Pimenov DY, Mia M, Gupta MK, Machado AR, Tomaz ÍV, Sarikaya M, Wojciechowski S, Mikolajczyk T, Kapłonek W (2021) Improvement of machinability of Ti and its alloys using cooling-lubrication techniques: A review and future prospect. J Mater Res Technol 11:719–753
8. Gupta MK, Song Q, Liu Z, Sarikaya M, Jamil M, Mia M, Singla AK, Khan AM, Khanna N, Pimenov DY (2021) Environment and economic burden of sustainable cooling/lubrication methods in machining of Inconel-800. J Clean Prod 287:125074
9. Nath C, Kapoor SG, DeVor RE, Srivastava AK, Iverson J (2012) Design and evaluation of an atomization-based cutting fluid spray system in turning of titanium alloy. J Manuf Process 14(4):452–459
10. Elsheikh AH, Abd Elaziz M, Das SR, Muthuramalingam T, Lu S (2021) A new optimized predictive model based on political optimizer for eco-friendly MQL-turning of AISI 4340 alloy with nano-lubricants. J

Manuf Process 67:562–578

11. Singh G, Pruncu CI, Gupta MK, Mia M, Khan AM, Jamil M, Pimenov DY, Sen B, Sharma VS (2019) Investigations of machining characteristics in the upgraded MQL-assisted turning of pure titanium alloys using evolutionary algorithms. Materials 12(6):999
12. Ghosh S, Rao P (2019) Comparison between sustainable cryogenic techniques and nano-MQL cooling mode in turning of nickel-based alloy. J Clean Prod 231:1036–1049
13. Sivalingam V, Zan Z, Sun J, Selvam B, Gupta MK, Jamil M, Mia M (2020) Wear behaviour of whisker-reinforced ceramic tools in the turning of Inconel 718 assisted by an atomized spray of solid lubricants. Tribol Int 148:106235
14. Rajeswari B, Amirthagadeswaran K (2017) Experimental investigation of machinability characteristics and multi-response optimization of end milling in aluminium composites using RSM based grey relational analysis. Measurement 105:78–86
15. Debnath S, Reddy MM, Yi QS (2014) Environmental friendly cutting fluids and cooling techniques in machining: a review. J Clean Prod 83:33–47
16. Poongavanam G, Sivalingam V, Prabakaran R, Salman M, Kim SC (2021) Selection of the best refrigerant for replacing R134a in automobile air conditioning system using different MCDM methods: A comparative study. Case Stud Therm Eng 27:101344
17. Gok A (2015) A new approach to minimization of the surface roughness and cutting force via fuzzy TOPSIS, multi-objective grey design and RSA. Measurement 70:100–109
18. Shukla A, Agarwal P, Rana R, Purohit R (2017) Applications of TOPSIS algorithm on various manufacturing processes: a review. Materials Today: Proceedings 4 (4):5320–5329
19. Gupta MK, Sood P, Singh G, Sharma VS (2018) Investigations of performance parameters in NFMQL assisted turning of titanium alloy using TOPSIS and particle swarm optimisation method. Int J Mater Prod Technol 57(4):299–321
20. Rao SR, Jeelani S, Swamulu V (2021) Multi-objective optimization using TOPSIS in turning of Al 6351 alloy, in: (Ed.)^(Eds.) IOP Conference Series: Materials Science and Engineering, IOP Publishing, pp. 012010
21. Thirumalai R, Seenivasan M, Panneerselvam K (2021) Experimental investigation and multi response optimization of turning process parameters for Inconel 718 using TOPSIS approach. Materials Today: Proceedings 45:467–472
22. Simic V, Karagoz S, Deveci M, Aydin N (2021) Picture fuzzy extension of the CODAS method for multi-criteria vehicle shredding facility location. Expert Syst Appl 175:114644
23. Kumar S, Gautam SK, Kumar A, Maithan R, Kumar A (2021) Sustainability assessment of different nanoparticle for heat exchanger applications: an intuitionistic fuzzy combinative distance-based assessment method. Acta Innovations 40:44–63
24. Badi I, Shetwan AG, Abdulshahed AM (2017) Supplier selection using COmbinative Distance-based ASsessment (CODAS) method for multi-criteria decision-making, in: (Ed.)^(Eds.) Proceedings of The 1st International Conference on Management, Engineering and Environment (ICMNEE), pp. 395–407

25. Chairman CA, Ravichandran M, Mohanavel V, Sathish T, Rashedi A, Alarifi IM, Badruddin IA, Anqi AE, Afzal A (2021) Mechanical and Abrasive Wear Performance of Titanium Di-Oxide Filled Woven Glass Fibre Reinforced Polymer Composites by Using Taguchi and EDAS Approach. Materials 14(18):5257
26. Asante D, He Z, Adjei NO, Asante B (2020) Exploring the barriers to renewable energy adoption utilising MULTIMOORA-EDAS method. Energy Policy 142:111479
27. Yazdani M, Torkayesh AE, Santibanez-Gonzalez ED, Otaghsara SK (2020) Evaluation of renewable energy resources using integrated Shannon Entropy—EDAS model. Sustainable Oper Computers 1:35–42
28. Alao MA, Ayodele TR, Ogunjuyigbe A, Popoola O (2020) Multi-criteria decision based waste to energy technology selection using entropy-weighted TOPSIS technique: The case study of Lagos. Nigeria Energy 201:117675
29. Feng J, Xu SX, Li M (2021) A novel multi-criteria decision-making method for selecting the site of an electric-vehicle charging station from a sustainable perspective. Sustainable Cities and Society 65:102623
30. Olson DL (2004) Comparison of weights in TOPSIS models. Math Comput Model 40(7–8):721–727
31. Jeet S, Barua A, Cherkia H, Bagal DK (2019) Comparative investigation based on MOORA, GRA and TOPSIS method of turning of nickel-chromium-molybdenum steel under the influence of low cost oil mist lubrication system. Int J Appl Eng Res 14(13):8–20
32. Keshavarz Ghorabaee M, Zavadskas EK, Turskis Z, Antucheviciene J (2016) A new combinative distance-based assessment (CODAS) method for multi-criteria decision-making.Economic Computation & Economic Cybernetics Studies & Research50 (3)
33. Gül S, Aydoğdu A (2021) Novel Entropy Measure Definitions and Their Uses in a Modified Combinative Distance-Based Assessment (CODAS) Method Under Picture Fuzzy Environment. Informatica 32(4):759–794
34. Ecer F, Pamucar D, Mardani A, Alrasheedi M (2021) Assessment of renewable energy resources using new interval rough number extension of the level based weight assessment and combinative distance-based assessment. Renewable Energy 170:1156–1177
35. Ijadi Maghsoodi A, Ijadi Maghsoodi A, Poursoltan P, Antucheviciene J, Turskis Z (2019) Dam construction material selection by implementing the integrated SWARA—CODAS approach with target-based attributes. Archives of Civil and Mechanical Engineering 19(4):1194–1210
36. Dhanalakshmi CS, Madhu P, Karthick A, Mathew M, Vignesh Kumar R (2020) A comprehensive MCDM-based approach using TOPSIS and EDAS as an auxiliary tool for pyrolysis material selection and its application.Biomass conversion and biorefinery:1–16
37. Torkayesh SE, Amiri A, Iranizad A, Torkayesh AE (2020) Entropy based EDAS decision making model for neighborhood selection: A case study in Istanbul. J Industrial Eng Decis Mak 1(1):1–11
38. Krishankumar R, Pamucar D, Deveci M, Ravichandran KS (2021) Prioritization of zero-carbon measures for sustainable urban mobility using integrated double hierarchy decision framework and EDAS approach. Sci Total Environ 797:149068

39. Roy J, Das S, Kar S, Pamučar D (2019) An extension of the CODAS approach using interval-valued intuitionistic fuzzy set for sustainable material selection in construction projects with incomplete weight information. Symmetry 11(3):393
40. No RKG, Niroomand S, Didehkhani H, Mahmoodirad A (2021) Modified interval EDAS approach for the multi-criteria ranking problem in banking sector of Iran. J Ambient Intell Humaniz Comput 12(7):8129–8148
41. Balasubramanian K, Nataraj M, Duraisamy P (2019) Machinability analysis and application of response surface approach on CNC turning of LM6/SiCp composites. Mater Manuf Process 34(12):1389–1400
42. Sivalingam V, Zhuoliang Z, Jie S, Baskaran S, Yuvaraj N, Gupta MK, Aqib MK (2021) Use of atomized spray cutting fluid technique for the turning of a nickel base superalloy. Mater Manuf Processes 36(3):373–380
43. Siddhpura M, Paurobally R (2012) A review of chatter vibration research in turning. Int J Mach Tools Manuf 61:27–47
44. Lee E, Nian C, Tarng Y (2001) Design of a dynamic vibration absorber against vibrations in turning operations. J Mater Process Technol 108(3):278–285
45. Sivalingam V, Zhao Y, Thulasiram R, Sun J, Nagamalai T (2021) Machining behaviour, surface integrity and tool wear analysis in environment friendly turning of Inconel 718 alloy. Measurement 174:109028
46. Bhatt A, Attia H, Vargas R, Thomson V (2010) Wear mechanisms of WC coated and uncoated tools in finish turning of Inconel 718. Tribol Int 43(5–6):1113–1121
47. Chavan V, Kadam S, Sadaiah M (2019) Performance of alumina-based ceramic inserts in high-speed machining of nimonic 80A. Mater Manuf Processes 34(1):8–17
48. Gupta S, Venkatesan K, Devendiran S, Mathew AT (2019) Experimental investigation of IN725 under different cooling environments using new tool holder. Mater Manuf Processes 34(6):637–647
49. Zhuang K, Zhu D, Zhang X, Ding H (2014) Notch wear prediction model in turning of Inconel 718 with ceramic tools considering the influence of work hardened layer. Wear 313(1–2):63–74
50. An Q, Cai C, Zou F, Liang X, Chen M (2020) Tool wear and machined surface characteristics in side milling Ti6Al4V under dry and supercritical CO2 with MQL conditions. Tribol Int 151:106511
51. Pal A, Chatha SS, Sidhu HS (2020) Experimental investigation on the performance of MQL drilling of AISI 321 stainless steel using nano-graphene enhanced vegetable-oil-based cutting fluid. Tribol Int 151:106508

Figures

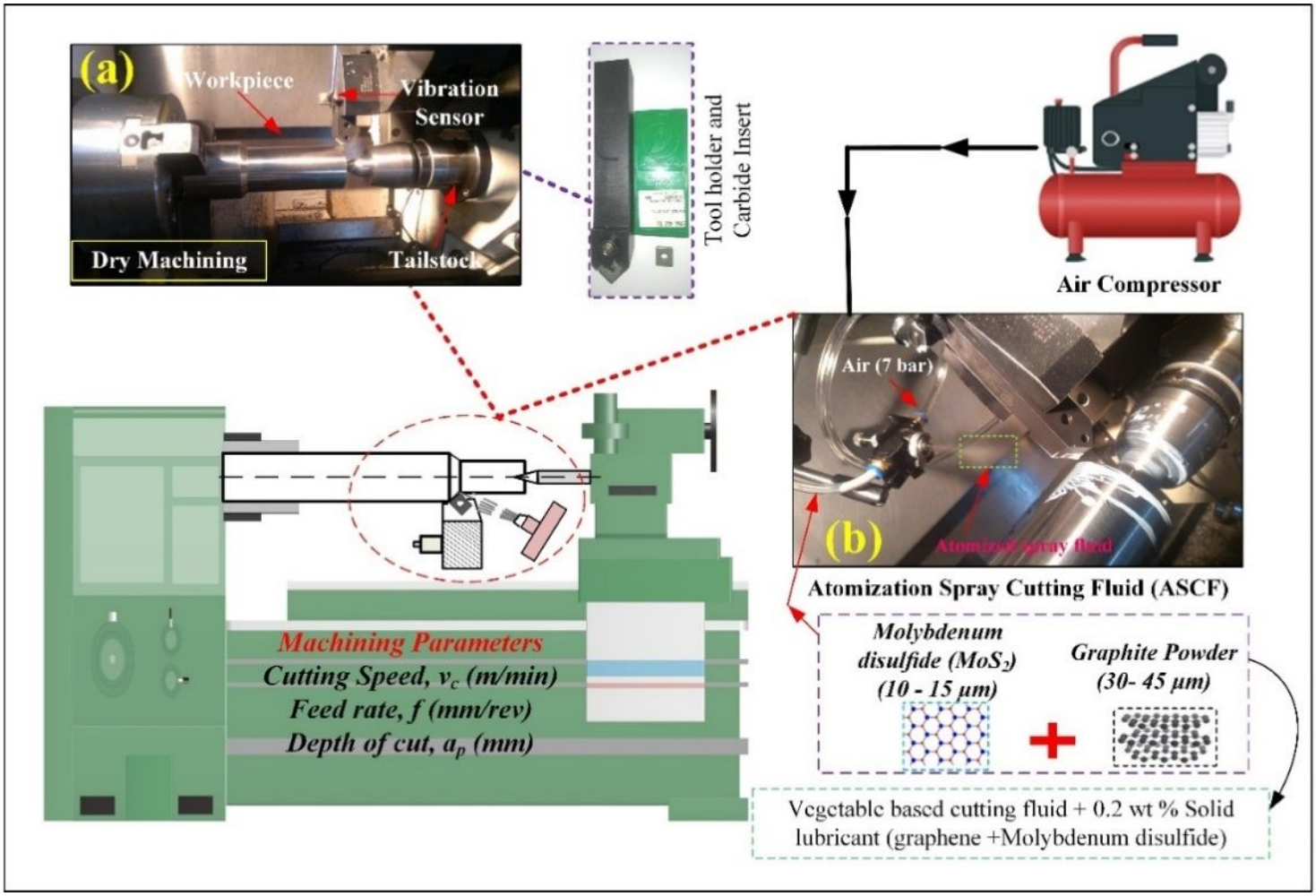

Figure 1

The schematic diagram for the dry and ASCF Machining

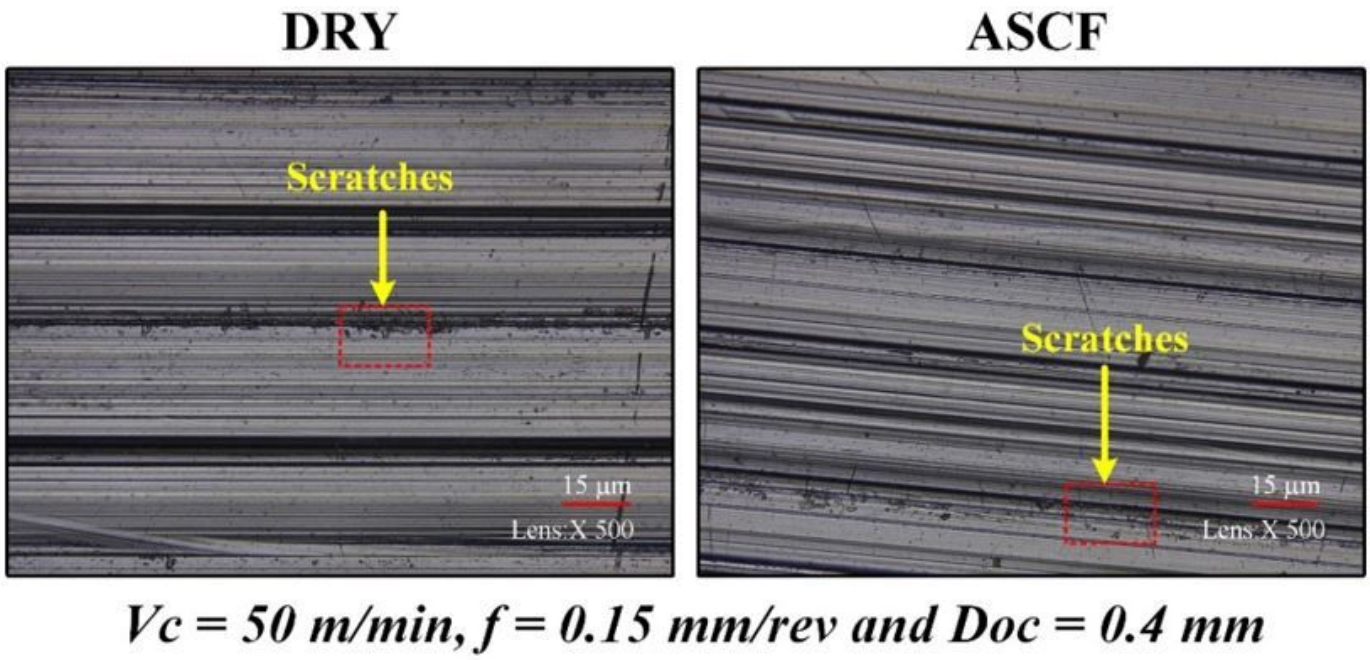

Figure 2

Optical Microscopic investigation of machined surface at the optimum condition of cutting speed 50m/min, feed rate of 0.15mm/min and depth of cut of 0.4 mm at both dry and ASCF condition

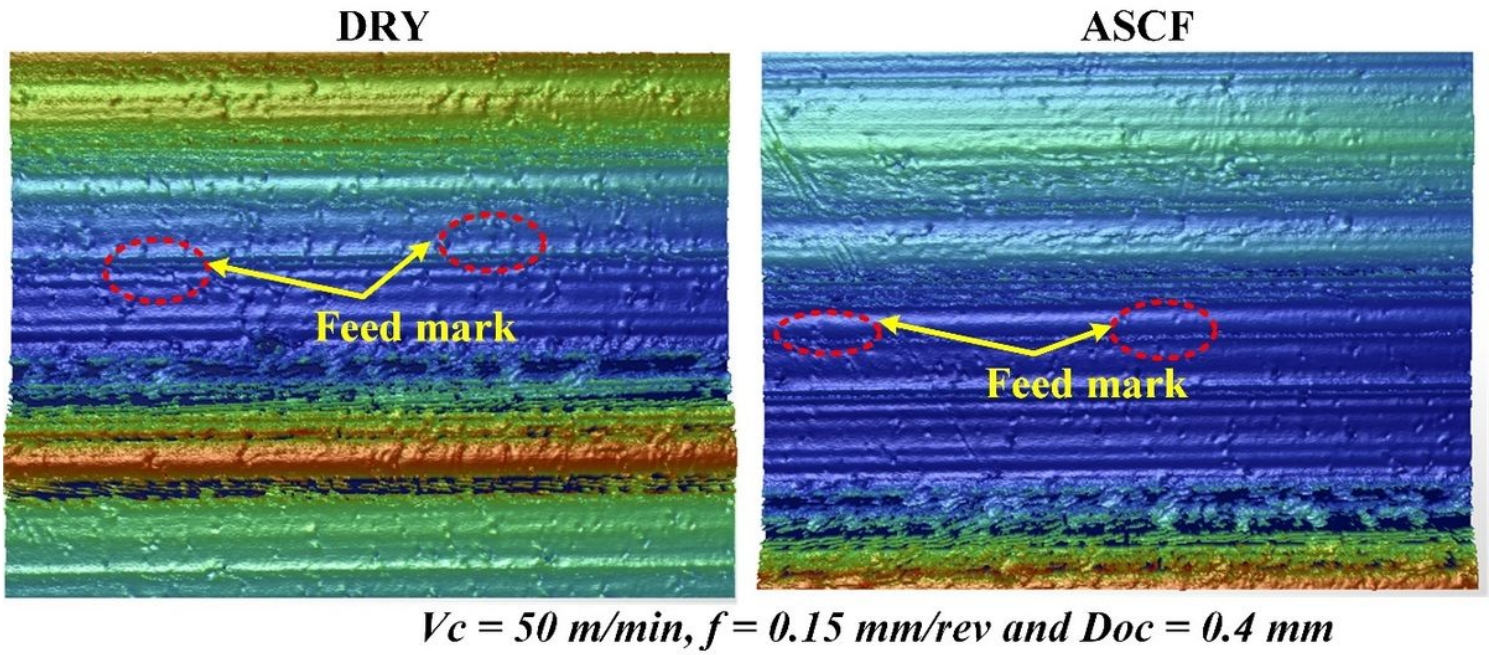

Figure 3

shows the 2D surface investigation of machined surface at the optimum condition of cutting speed 50m/min, feed rate of 0.15mm/min and depth of cut of 0.4 mm at both dry and ASCF condition

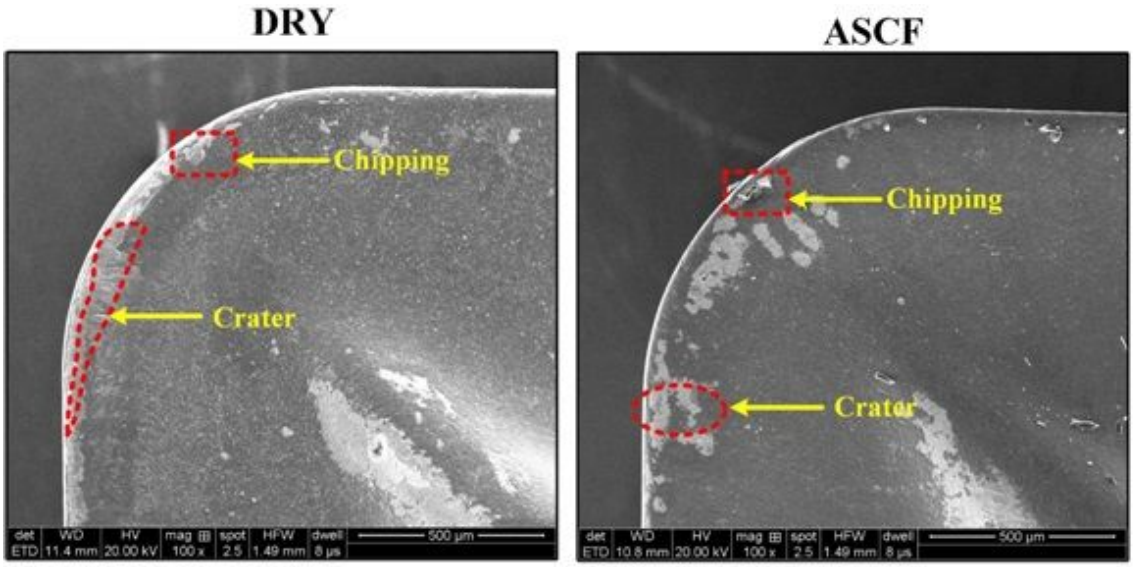

Figure 4

SEM investigation of tool wear at the optimum condition of cutting speed 50m/min, feed rate of 0.15mm/min and depth of cut of 0.4 mm at both dry and ASCF condition.